Solving the Inverse Problem of Magnetisation - Stress Resolution

S.G.H. Staples[†], C.Ives[†], C. Vo[§] , D. Cowell[§] , S. Freear[§] , B. T. H. Varcoe[†*]
[†] *University of Leeds, Experimental Quantum Information, Department of Physics and Astronomy and*
[§] *University of Leeds, Department of Electrical Engineering*
(Dated: January 8, 2013)

Magnetostriction in various metals has been known since 1842, recently the focus has shifted away from ferrous metals, towards materials with a straightforward or exaggerated stress magnetostriction relationship. However there is an increasing interest in understanding ferrous metal relationships, especially steels, because of its widespread use in building structures, transportation infrastructure and pipelines. The aim of this paper is to solve the inverse problem of determining stress from an observed magnetic field which implies a given magnetic structure and to demonstrate that theoretical calculations using a multi-physics modeling technique agree with this experimental observation.

1. INTRODUCTION

Understanding the magnetic properties of steel, when subjected to earths magnetic field, is becoming a key requirement in order to utilise passive magnetic field measurements for condition monitoring of steel structures. The magnetostriction of steel and magnetisation caused by stress in steel have long been known, but as yet only partially understood and exploited. When stress is applied to a ferrous structure, for example a steel bar, the magnetisation of the steel changes as a function of stress and this causes a change in the magnetic field around the structure. Figure 1 shows a simple scheme relating stress $\boldsymbol{\sigma}$ which is produced by force $\boldsymbol{F}$, magnetisation $\boldsymbol{M}$ and induced field $\boldsymbol{B}$, which has been the basis for modeling this phenomena [1][2][3][4]. It is the aim of this paper to demonstrate the inverse problem of resolving stress in material by the observed magnetic field, and to do this it is necessary to validate multi-physics modeling of magnetic field and related stress with experimental observations, this will show that Figure 1 is a valid assumption.

Magnetostriction is an effect first discovered by Joule in 1842. The Villari effect was discovered by Villari[5] in 1865, and is the inverse of the Joule effect. The first major study of this was by Lee[6], later work by Tremolet de Lacheisserie [7] has provided a wider study of the effects of magnetostriction and its applications. Magnetostriction has been modeled theoretically by Jiles, Atherton and Sablik [8][9] and experimental results [10] have been used to demonstrate the validity of the model. Work by Atherton and Jiles has shown experimental relevance on pipeline materials [11][12][13][14]. Further work by Jiles and Li [15][16] has refined the theory. Jiles et al developed further experimental work to dependence on steel composition [17] and crack size [18]. Recent studies by Viana[19] and Li [20] have improved on this model, notably in the modeling of the anhysteric form of stress magnetisation and the asymmetry of the tension and compression modes. From this work it is clear that stress and magnetisation are related, and in order to determine the stress regime in steel that is subjected to cyclic stresses, it is necessary to understand the magnetic field that is generated as a result. Jiles, Atherton and Sablik [8][9], have provided a comprehensive theoretical treatment of magnetostriction as applied to ferrous materials. This has been named by Jiles as the 'theory of approach', whereby the magnetisation in ferrous material tends to the anhysteric during successive cycles of stress. The theory has successfully modeled earlier experimental data, different material to that studied in this paper, and the theoretical system is encapsulated in the following expression[9]

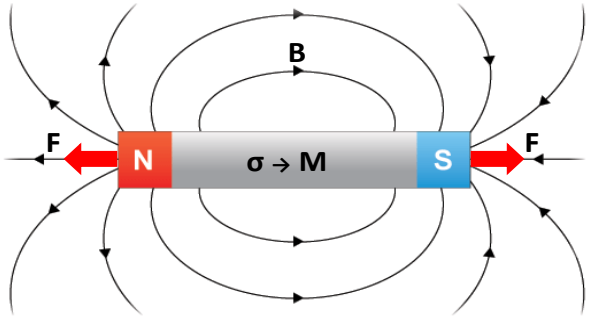

FIG. 1: Simple schematic of Stress $\boldsymbol{\sigma}$ produced by force $\boldsymbol{F}$, magnetisation $\boldsymbol{M}$ and Induced field $\boldsymbol{B}$

$$\frac{dM}{d\sigma} = \frac{1}{\epsilon^2}(\sigma \pm \eta E)(1-c)(M_{an} - M_{irr}) + c\frac{dM_{an}}{d\sigma} \quad (1)$$

where M is magnetisation, σ is stress, ϵ is a property of the material related to Young's Modulus, η and c are constants that reflect the ability of magnetic domains to become magnetised, M_{an} is the anhysteric magnetisation and M_{irr} the irreversible part of magnetisation. This equation can be solved numerically, to give a relationship between stress and magnetisation. Figure 2 shows a typical solution using data from Jiles[9]. The solution

*Electronic address: py10sghs@leeds.ac.uk

presented, shows that irreversible magnetisation can be expected with steel that is stress cycled, the magnetisation will tend towards the anhysteric value with repeated stress cycles, whether the material has zero magnetisation or starts from some finite value, providing that there is some external magnetic field present, which could be earths magnetic field. Interestingly the anhysteric curve has a magnetisation that is always greater than zero, thus stress cycling will provide a residual positive magnetic memory. However, as can be observed from the solution, this provides a relationship with M/M_s, and this has to be further transformed into a relationship with the induced magnetic field B, surrounding the object or system under study. For complicated structures such as steel rails, beams or cylinders this requires further understanding of the structure of the magnetic field surrounding the object, hence the available theory is difficult to use directly. Wang et al have developed theoretical and experimental work in this direction, [2][3][4]. Demonstrating that the magnetic field due to a stress concentration regime is of a predictable and repeatable pattern will aid the interpretation of complex data from steel structures. The experiments in the next sections, were conducted in order to map the magnetic field due to tensile stress and to compare it to that theoretically calculated using a multi-physics modeling tool (COMSOL). Understanding the magnetic field behaviour, and possessing the ability to characterise and model it, is a key step to being able to use stress magnetisation modeling and experimental data to determine the stress level in a given steel component based upon its magnetic field. Being able to parametrise stress - magnetisation from observation of magnetic field will facilitate the use of field measurement by magnetometry in non-invasive testing of steel materials.

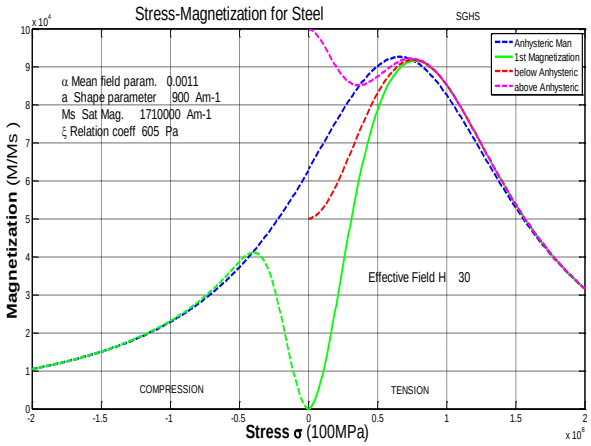

FIG. 2: Solution of the Jiles Atherton Sablik equation

2. EXPERIMENTAL METHOD

2.1. Model development from Experimental data

In order to understand the magnetic field surrounding a stressed steel object, a simple relation of stress - magnetic field needs to be developed, that can then be used in a multi-physics modeling tool to predict the magnetic field. In order to do this samples of steel need to be stress tested using the techniques described in the next section. This is based upon modeling the entire observed magnetic field B as a function of the applied stress σ, that is the relationship of $B = \mu_0(H + M)$ is implicit in this operation, where H is the total applied field which will be the sum of H_e (earth's field) and H_σ the field due to stress, and M is the magnetisation of the steel due to this effective stress field (Villari effect). The stress induced field B is then modeled as a function of σ, using the simple relationship of $B = \alpha\sigma^2 + \beta\sigma + \gamma$. This leads to an experimental derived relationship between stress and magnetic field, which can then be modeled as a curve fit and used in COMSOL modeling software. The details of this are described in the next section.

2.2. Experimental Method

Two steel samples, comprised of 45# grade steel plate, see table II for composition and III for strength properties, were subjected to tensile stress, using a RDP Howden tensile stress testing machine. The two respective samples were a 20 mm width rectangular bar, and a 4 mm width dumbbell sample as shown in Figure 5. The 4 mm sample was fabricated in accordance with EN8 - stress testing of metals[21]. For the case of the 20 mm bar, see table I.

TABLE I: Curve fit parameters 45# Steel 20 mm bar

Curve	α	β	γ
Forward	3.966×10^{-5}	7.403×10^{-18}	0
Reverse	-1.324×10^{-5}	0.001859	4.173

Figure 3 shows a curve fit solutions using experimental data, for five different width samples, that is used in this manner. It can be readily observed that there is a direct correlation between the sample width and the overall intensity of remanent magnetisation, i.e. overall height on the vertical axis. The correlation can be readily demonstrated by plotting sample width against remanent magnetisation. Figure 4 shows the correlation between sample width and magnetisation, termed magnetic memory, can be regarded as linear, in this case the correlation has been adjusted to pass through zero magnetisation at zero width.

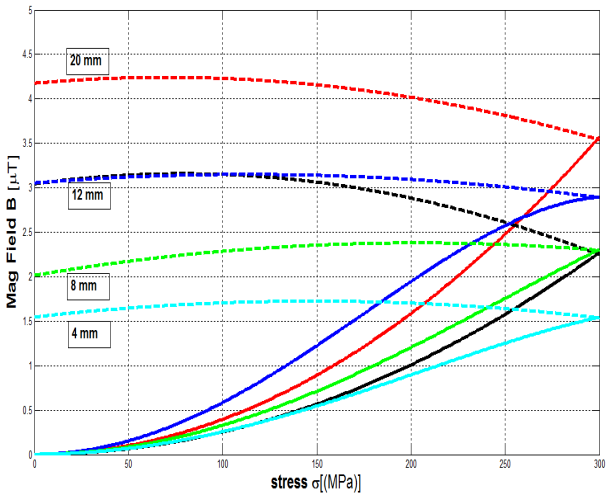

FIG. 3: Curve Fit of Stress - Magnetisation, showing Variation of Magnetic Memory with Sample Width

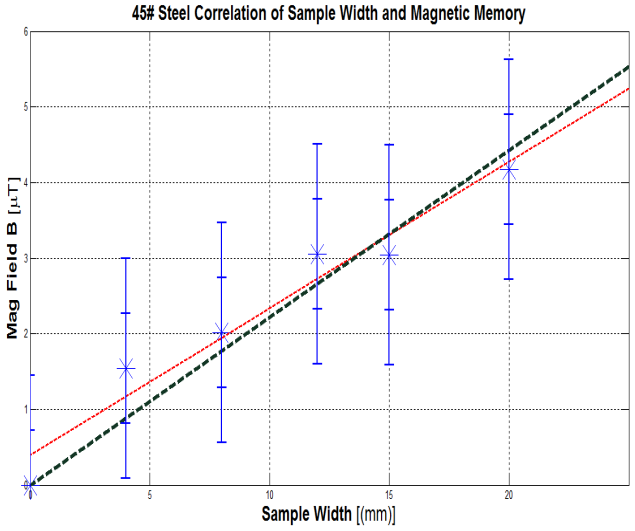

FIG. 4: Correlation of Sample Width (mm) with Magnetic Memory Error bar set at 0.5 SD (inner) 1 SD (outer) Line of best fit forced to zero

Figure 3 demonstrates the increase in magnetic memory with sample width, indicating that the property being measured is the bulk magnetisation, and thus the field being measured is a direct property of the geometry of the steel body. This is in agreement with the work by Wang et al [2][3][4]. The samples were prepared,

TABLE II: Composition of 45# Steel %wt

C	Si	Mn	Cr	Ni	Others
0.42-0.50	0.17-0.37	0.50-0.80	< 0.25	< 0.25	< 0.035

TABLE III: Properties of 45# Steel

Tensile Strength (N/mm)	Yield point (N/mm)
570	295

before any testing by a degaussing technique, which allowed them to be demagnetised. Then in the first set of experiments they were subjected to a stress cycle using the tensile stress machine, up to a maximum force of 10 KN. This subjected the sample to a maximum stress of 200-300 MPa dependent upon their respective cross sectional area. The force was applied along the long axis of each sample at a constant rate up to the maximum. Stress and magnetic field (X,Y,Z direction) were recorded against time, the sample alignment as per Figure 6. The results of this stage were then used to produce a stress-magnetisation curve for both tension and relaxation which was discussed in the previous section. In the second set of experiments the demagnetised samples were placed on a coordinate grid and the respective magnetic field magnitudes were measured for 70 positions, in order to provide a surface mapping of magnetic field around the sample. The directions of magnetic field are shown in Figure 6. The magnetic field at a given point was measured using a Bartington fluxgate magnetometer. The samples were subjected to a tensile stress of approximately 170 MPa (20 mm sample) and 300 MPa (4 mm sample), by applying a force along the long axis of each sample using the tensile stress machine. The magnetic field mapping was then repeated with the stress cycled sample, thus the magnetic field due to the magnetisation caused by stress could be determined as the difference of the two mappings. Figure 6 shows the 20 mm sample undergoing a stress test. Each sample was subjected to the required force to give the respective stresses, and then the tension was released to zero, thus providing one tension relaxation cycle. The magnetic field was measured on a plane for three successive vertical heights (27 mm, 110 mm and 155 mm), such that that vertical variation of magnetic field could also be inferred.

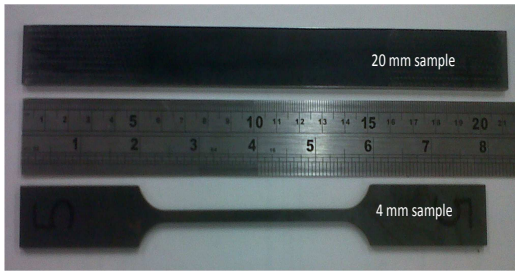

FIG. 5: Typical Test samples used in Experiment

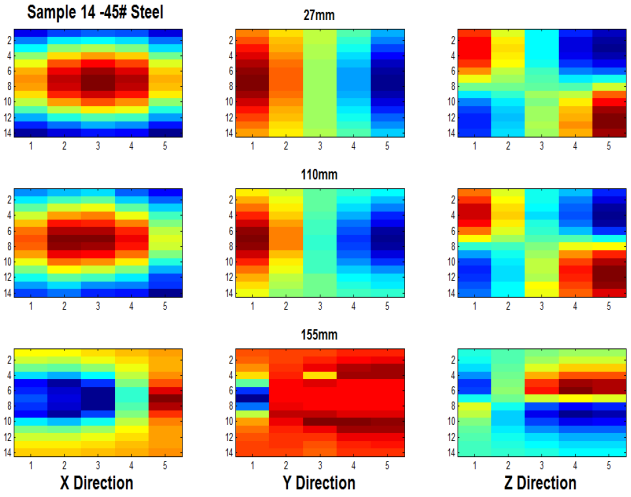

FIG. 7: Mapping of Measured Magnetic Field for 20 mm bar sample, at heights of 27mm, 100mm and 155mm

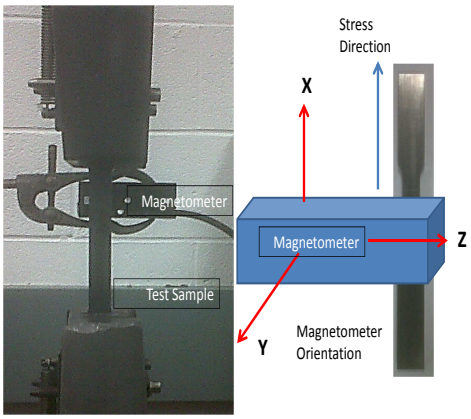

FIG. 6: Subjecting the 20 mm sample to tensile stress

3. RESULTS

The results of the experiment are coordinate mappings of magnetic intensity. Figure 7 shows the magnetic field mapping results for the 20 mm steel bar.The 20 mm bar shows a clear pattern for the two lower levels, both having a very similar orientation for the X , Y, and Z magnetic field directions. The pattern is less distinct for the 4 mm case, only the middle level showing a field orientation similar to that of the 20 mm case. The 4 mm bar has much less metal surface area, only 20% of the 20 mm case, which considerably weakens the magnetic signal, albeit there is increased magnetisation due to a higher stress level. The field patterns show that

i. in the X direction, the high intensity field is at the center of the bar, low intensity at the sides

ii. in the Y direction intensity decreases as distance from the bar increases

iii. in the Z direction there are diagonal symmetry of intensity, indicating the fields change direction

All of this is consistent with looped field lines that are flowing from poles at either end of the bar, to the opposite pole in the centre of the bar.

4. COMPUTATIONAL MODEL

In order to explore how the samples behave under stress, a multi-physics modeling programme, COMSOL, was used to model the stress distribution in the two samples, using a finite element technique. The process is broken down into a series of steps in order to achieve a model of the stress - magnetisation relationship.

Firstly, the geometry of the given specimen is modeled, using a 3D drawing tool, this was in fact the same one used in the fabrication of the sample from plate steel. Once the 3D model is available it can be imported into the multi-physics software, at this stage the air space around the ferrous specimen has to be included in the model. Figure 8 shows the 3d model of the steel bar sample used in this experiment.

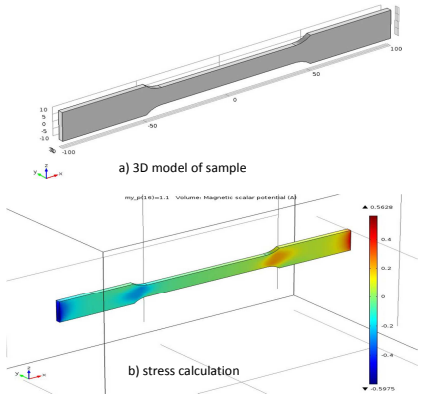

FIG. 8: a) 3d model of steel sample b) Stress calculation and mapping

The material properties are needed to calculate tensile stress in the sample, table II for composition and III for strength properties, have been shown in previous experimental section. The software models of stress using a finite element method with the modeled sample meshed into small regions.

Once the stress distribution has been calculated, then a stress - magnetisation relationship can be used in the COMSOL model. This has been obtained empirically, as described in the experimental section, by stress testing of similar samples and determining the stress-magnetisation curve, which is a curve fit of the experimental data. The resultant magnetic field around stress concentration zones in the sample can thus be mapped, in order to visualise the field, an example of this is shown in figure 9. From this the magnetic intensity images were developed, for the the three perpendicular field directions X,Y and Z.

5. DISCUSSION AND COMPARISON OF RESULTS-THEORETICAL MODEL

The results of the experiments, and the calculated results from COMSOL can now be compared on the same basis. Figure 10 shows the magnetic field mapping comparison results for the 20 mm steel bar, alongside the field calculated by the COMSOL model. Allowing for the resolution the images are strikingly similar, with the COMSOL and experiment showing corresponding images in the three planes XYZ. It is noted that due to the stress - magnetic field modeling process that there will be a scaling factor between the experimental observations and the COMSOL model, as can be seen the two scales are not the same, but there is a linear correspondence between the two, this will be explored further in later experiments.

The magnetic field mapping comparison is discussed

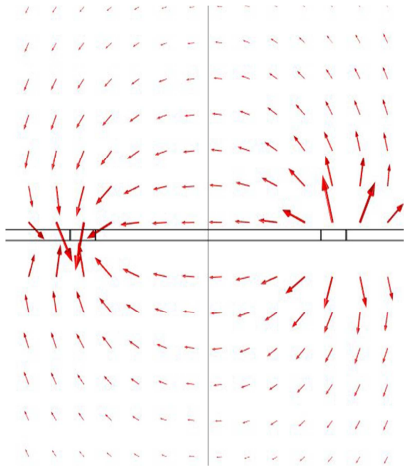

FIG. 9: Orientation of magnetic field

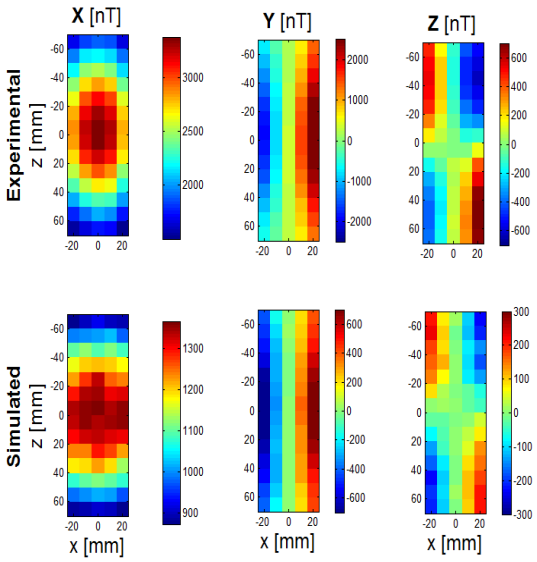

FIG. 10: Mapping of Measured Magnetic Field for 20mm bar sample compared to that calculated by COMSOL model

as

i. in the X direction, the field lines approach the south pole from the the north pole, thus when viewed in the X direction the field lines are closer together at the centre of the bar and widen out, creating a high intensity zone

ii. in the Y direction the field lines converge at the south pole from the north pole, as the Y distance increases then the lines get further apart, creating

an intensity gradient

iii. in the Z direction, field lines leave the North pole in opposite directions at each corner thus there are diagonal symmetry of intensity, indicating the fields change direction

As can be observed the magnetic field intensity corresponds to the expected field orientation on each major plane, again strong evidence that the applied stress has a consistent orientation of magnetic field. The experimental and model images show an excellent correspondence, thus there is objective evidence that the modeled stress concentration zones have the same magnetic field image as those obtained by experiment, thus the multi-physics model is validated. This will lead to the model being used to tackle the inverse problem of resolving stress from a given magnetic field pattern.

6. CONCLUSIONS

The experimental and theoretical calculation discussions in the previous sections show excellent agreement, and give strong indication that the magnetic field created due to a bar being subjected to a stress cycle corresponds to the initial assumptions. The poles are formed at either end of the stress concentration zone, in the cases examined this was the entire length of the sample in between the jaws of the tensile stress tester. An interesting development would be to introduce known defect or stress concentration zones in this region to see how the field changes, this will be done in a further set of experiments. This gives an important indication of the magnetic field orientation around an area of stress concentration in a steel component, and allows magnetic field data to be interpreted to predict both stress concentration and areas of abnormal condition. This is the first step in resolving the inverse problem of stress determination for a given steel structure from its surrounding magnetic field. Further work will include the development of the linear correspondence between experimental and model, and of stressed bars which have manufactured defect, allowing the magnetic field - stress relationship of defect zones to be analysed.

Acknowledgments The work in this paper is possible due to the funding by Speir Hunter Ltd.

[1] S. Bao, T. Erber, S. A. Guralnick, and W. L. Jin, Strain (Interantional journal for experimental mechanics) **47**, 372 (2011).
[2] Z. D. Wang, K. Yao, B. Deng, and K. Q. Ding, NDT E International **43**, 354 (2010).
[3] Z. D. Wang, K. Yao, B. Deng, and K. Q. Ding, NDT E International **43**, 513 (2010).
[4] Z. D. Wang, B. Deng, and K. Yao, Journal of Applied Physics **109**, 083928 (2011).
[5] Villari, Annals of Physics (1865).
[6] E.W.Lee, Rep. Prog. Phys. **18**, 184 (1955).
[7] E. d. T. d. Lacheisserie, *Magnetostriction - Theory and Applications of Magnetoelasticity* (CRC Press Boca Raton, 1993).
[8] M.J.Sablik, IEEE Transactions on Magnetics **33**, 2958 (1997).
[9] D. Jiles, J. Phys. D: Appl. Phys. **28**, 1537 (1995).
[10] D. J. Wood and M. J. Craik, J. Phys. D: Appl. Phys. **3**, 1009 (1970).
[11] D. Atherton and D. Jiles, IEEE Transactions on Magnetics **19**, 2021 (1983).
[12] D. Jiles and D. Atherton, J. Phys. D: Appl. Phys. **17**, 1265 (1984).
[13] D. Atherton, D. Jiles, C. Welbourn, L. Reynolds, and J. Scott-Thomas, IEEE Transactions on Magnetics **20** (1984).
[14] D. Atherton, D. Jiles, L. Coathup, L. Longo, C. Welbourn, and A. Teitsma, IEEE Transactions on Magnetics **19** (1983).
[15] D. Jiles and L. Li, IEEE Transaction on Magnetics p. 3037 (2003).
[16] D. C. Jiles and L. Li, Journal of Applied Physics **95**, 7058 (2004).
[17] D. Jiles and M. Devine, IEEE Transactions on Magnetics **32**, 4740 (1996).
[18] D. Jiles and Y. Bi, IEEE Transactions on Magnetics **34**, 2021 (1998).
[19] A. Viana, J. L. Coulomb, L. L. Rouve, and G. Cauffet, Journal of Magnetism and Magnetic Materials **322**, 186 (2010).
[20] J. Li and M. Xu, Journal of Applied Physics **110**, 063918 (2011).
[21] A. International, ASTM Standards (2012).